Polar amplification as an inherent response of a circulating atmosphere: results from the TRACMIP aquaplanets

Rick D. Russotto[1] **and Michela Biasutti**[1]

[1]Lamont-Doherty Earth Observatory of Columbia University

[1]61 Route 9W, Palisades, NY 10964

Key Points:

- Polar amplification occurs robustly in the TRACMIP aquaplanet simulations
- Moisture transport mediates the contributions of different forcing and feedback components to polar amplification
- The instantaneous CO_2 forcing and water vapor feedback are the largest contributors to polar amplification

Corresponding author: Rick Russotto, `russotto@ldeo.columbia.edu`

Abstract

In the TRACMIP ensemble of aquaplanet climate model experiments, CO_2-induced warming is amplified in the poles in 10 out of 12 models, despite the lack of sea ice. We attribute causes of this amplification by perturbing individual radiative forcing and feedback components in a moist energy balance model. We find a strikingly linear pattern of tropical versus polar warming contributions across models and processes, implying that polar amplification is an inherent consequence of diffusion of moist static energy by the atmosphere. The largest contributor to polar amplification is the instantaneous CO_2 forcing, followed by the water vapor feedback and, for some models, cloud feedbacks. Extratropical feedbacks affect polar amplification more strongly, but even feedbacks confined to the tropics can cause polar amplification. Our results contradict studies inferring warming contributions directly from the meridional gradient of radiative perturbations, highlighting the importance of interactions between feedbacks and moisture transport for polar amplification.

Plain Language Summary

In both observations and computer model simulations, the polar regions (especially the Arctic) warm more than the rest of the world in response to increased greenhouse gas concentrations. Scientists disagree on the reasons for this "polar amplification" of warming. The melting of ice floating in the ocean, which lets more sunlight be absorbed, is often given as an explanation, but climate models with no sea ice also display polar amplification. We ran hundreds of experiments with a simple climate model in order to understand the reasons for polar amplification in more complex models that lack sea ice. We found that the main reason is that the atmosphere transports energy from the tropics to the poles, so much so that even processes that initially add energy mostly to the tropics cause polar amplification. Our methods produce different explanations from past studies because they did not fully account for this movement of energy.

1 Introduction

Despite many years of research, the causes of the polar amplification of warming caused by increased greenhouse gases remain a topic of debate. This phenomenon of greater warming at the poles is often attributed to feedbacks involving the loss of polar ice, due to the exposure of less reflective underlying surfaces (Hall, 2004) or interactions between

sea ice and ocean heat storage and release (Dai et al., 2019). However, polar amplification has also been found in global climate model (GCM) simulations with fixed albedo (Alexeev et al., 2005; Graversen & Wang, 2009), indicating that ice-albedo feedbacks are not necessary for polar amplified warming. The opposing sign of the lapse rate feedback at low versus high latitudes (Pithan & Mauritsen, 2014) and cloud feedbacks (Vavrus, 2004) have also been cited as contributing factors to polar amplification.

In the context of this body of work, the Tropical Rain belts with an Annual cycle and Continent Model Intercomparison Project (TRACMIP; Voigt et al. (2016)) is well positioned to provide useful insights into polar amplification, as it provides the physics of complex models but a very idealized configuration. TRACMIP consists of aquaplanet GCM experiments with a seasonal cycle, a slab ocean with 30 m mixed layer depth, and a prescribed ocean heat transport in the form of q-fluxes approximating that of the real Earth in the zonal mean. Clouds and water vapor are allowed to interact with atmospheric radiation in all 12 models considered in this study, but there is no sea ice in any of the models. We consider the difference between the AquaControl experiment, with a CO_2 concentration of 348 ppmv, and the Aqua4xCO2 experiment, in which CO_2 is quadrupled, similar to the Abrupt4xCO2 experiment of the Coupled Model Intercomparison Project (CMIP; Taylor et al. (2012)). Polar amplification in response to quadrupled CO_2 occurs in 10 out of 12 full-radiation GCMs (Fig. 1a,f), making this a useful multi-model test case to attribute the causes of polar amplification in the absence of surface ice.

This study aims to account for the polar amplification in the TRACMIP Aqua4xCO2 ensemble, despite the lack of sea ice, and to comment on the behavior of the meridional temperature gradient in GCMs and energy balance models. We attribute the contributions of different radiative feedbacks, rapid adjustments, and the instantaneous CO_2 forcing to the polar amplification in TRACMIP. Some studies (Pithan & Mauritsen, 2014; Goosse et al., 2018; Stuecker et al., 2018) have done this attribution by calculating the change in radiation at the top of atmosphere (TOA) from each feedback, then diagnosing a surface warming contribution, for example by inverting the surface temperature radiative kernel (Pithan & Mauritsen, 2014) or normalizing by the global mean Planck feedback (Goosse et al., 2018). These studies have typically found that polar amplification is primarily due to local, high-latitude forcings and feedbacks, particularly the lapse rate feedback, which is positive at high latitudes and otherwise negative, with the surface albedo feedback playing a secondary role. Other studies (Hwang & Frierson, 2010;

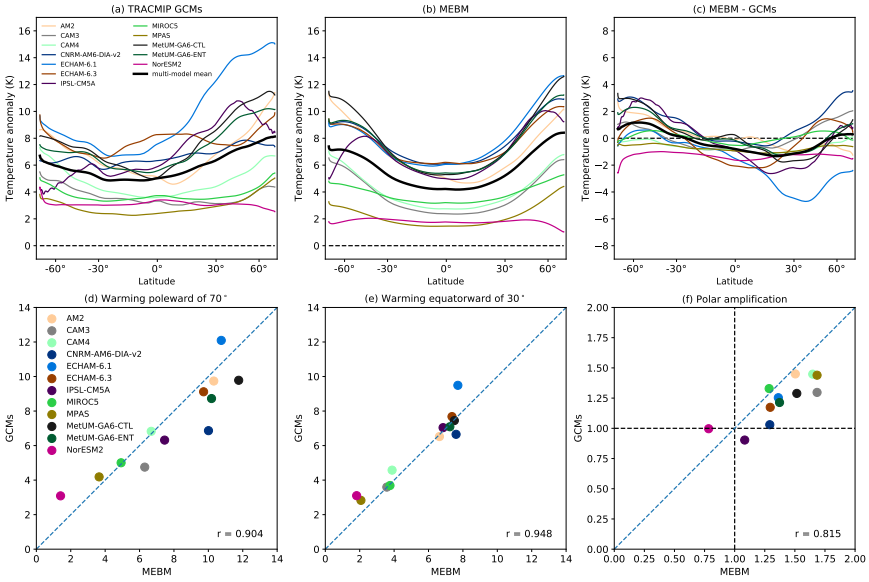

Figure 1. Zonal mean surface temperature change in (a) TRACMIP GCMs, (b) moist energy balance model, and (c) difference, and scatter plots of warming in MEBM vs. GCMs averaged over high latitudes (d), tropics (e), and ratio of high latitude to global mean warming (f). Refer to model names in Table 3 of Voigt et al. (2016).

Hwang et al., 2011; Roe et al., 2015; Bonan et al., 2018; Armour et al., 2019) have run attribution experiments in which forcings and feedbacks are perturbed in a moist energy balance model (MEBM) which allows for interactions between the feedbacks and energy transport. Hwang and Frierson (2010) demonstrated that the MEBM well reproduces poleward energy transport in coupled models, and found cloud feedbacks to be the largest source of inter-model spread. Perturbing the feedback parameter in the MEBM either in the tropics or the poles, either with idealized perturbations (Roe et al., 2015) or with CMIP5-based feedbacks (Bonan et al., 2018), indicates that uncertainty in tropical feedbacks strongly transmits the inter-model spread in warming to the poles, while the effects of polar feedbacks are felt more locally.

We apply the MEBM approach to the TRACMIP ensemble, combining different methodologies in a way not previously done to study the roles of specific forcings and feedbacks in enhancing tropical versus polar warming. We show that the roles of various feedbacks, particularly the water vapor feedback, in polar amplification are much different from what has been described in the existing literature when energy transport is accounted for. We also find striking consistency in the ratio of contributions to tropical versus polar warming across models and feedbacks, with positive feedbacks in general causing polar amplification. This suggests that polar amplification of warming is an inherent property of an atmosphere that diffuses moist static energy (MSE), as previously suggested by Merlis and Henry (2018).

2 Methods

2.1 Setup of moist energy balance model experiments

Energy balance models (EBMs) are one-dimensional representations of the zonal mean climate that diffuse energy down-gradient (e.g., North et al., 1981). MEBMs, first introduced by Flannery (1984), are an extension of classical EBMs and diffuse moist static energy (MSE) rather than temperature. There are two MEBM versions commonly used today: a climatological version, used, *e.g.*, by Hwang and Frierson (2010), Hwang et al. (2011), and Frierson and Hwang (2012), and a perturbation version, used by Roe et al. (2015), Siler et al. (2018), Bonan et al. (2018), and Armour et al. (2019). The climatological MEBM diffuses absolute MSE and highly simplifies radiative feedbacks. The perturbation MEBM diffuses anomalous MSE and allows feedbacks to vary with latitude.

We use the perturbation MEBM because it allows for independent specification of LW feedbacks, and because it allows feedbacks to interact with local temperature changes.

The diffusion of MSE in the perturbation MEBM, neglecting changes in ocean heat uptake which do not apply here, is expressed by (*e.g.* Bonan et al., 2018):

$$R_f(x) + \lambda(x)T'(x) + \frac{p_s}{a^2 g} D \frac{\mathrm{d}}{\mathrm{d}x}\left[(1-x^2)\frac{\mathrm{d}h'(x)}{\mathrm{d}x}\right] = 0. \tag{1}$$

Here $R_f(x)$ is the effective radiative forcing associated with the CO_2 increase, which is defined as the instantaneous CO_2 forcing plus the sum of the changes to the TOA energy balance, known as rapid adjustments, that occur when atmospheric temperature, humidity, and clouds respond to the CO_2 increase before the sea surface temperature has a chance to respond (Myhre et al., 2013). λ is the net radiative feedback; T'_s is the surface temperature anomaly; p_s is the surface pressure; a is the Earth's radius; g is the gravitational acceleration; D is the diffusivity; and $h' = c_p T' + L_v q'$ is the perturbation near-surface MSE, where c_p is the heat capacity of air at constant pressure, L_v is the latent heat of vaporization of water, and q' is the perturbation specific humidity. The MEBM is run to equilibrium starting from a uniform temperature profile, with specified values of $R_f(x)$ and $\lambda(x)$. We use a value of 9.6×10^5 m^2 s^{-1} for D, following Bonan et al. (2018), and a relative humidity of 80% as is typical for these experiments. We also tried a diffusivity of 1.06×10^6 m^2 s^{-1}, following Hwang and Frierson (2010), and found that it did not much affect T'_s at equilibrium (not shown). For our "control" MEBM experiment, we calculate R_f and λ by regressing the total anomaly in top of atmosphere (TOA) radiative imbalance against the surface temperature anomaly at each latitude in Aqua4xCO2 - AquaControl, following Gregory et al. (2004). The slope of this regression is λ, and the intercept is R_f. Anomalies are calculated in each month of Aqua4xCO2 relative to the climatology for that month in AquaControl, and then the mean of each year is taken before regression to eliminate effects of changes in the seasonal cycle. Note that feedbacks calculated this way are defined against zonal mean, rather than global mean, temperature change (see Feldl and Roe (2013) for a discussion of this distinction).

For each physical property of interest, including cloud cover, humidity, and atmospheric temperature, we calculate the change in TOA radiation using established methods and regress it against surface temperature anomalies using the Gregory method. The intercept of each regression is the rapid adjustment, or the contribution to the effective radiative forcing, and the slope is the feedback. We calculate rapid adjustments and feed-

backs for different physical processes in each TRACMIP model individually, then "turn off" each of them one at a time in the perturbation MEBM by subtracting each rapid adjustment from R_f and subtracting each feedback from λ. The effect of turning off each process on the meridional temperature gradient, relative to a control MEBM run forced with the effective radiative forcing and total radiative feedback, represents the contribution of that process to polar amplification (with the sign reversed). Note that turning off the Planck feedback results in a runaway greenhouse effect due to a positive total feedback, so instead we reduce the strength of this feedback by 10%. Perturbing the feedback by 5% and 15% instead results in an overall warming that scales exponentially with the amount reduced (not shown), but the ratio of polar to tropical differences in T_s' is similar in all three cases.

In its control configuration, the perturbation EBM exhibits a pattern of warming amplified at the poles similar to that seen in the GCMs themselves, albeit the MEBM warming is smoother and more hemispherically symmetric (Figure 1b-c). There are strong correlations, with correlation coefficient r at least 0.81, between the MEBM- and GCM-derived warming averaged over high latitudes (poleward of 70°; Figure 1d), the tropics (equatorward of 30°; Figure 1e), and for the polar amplification (warming poleward of 70° divided by global mean warming, following Hwang et al. (2011); Figure 1f). The good agreement between the MEBM and GCMs shown in Figure 1 gives us confidence that attribution experiments in which rapid adjustments and feedbacks are perturbed individually in the MEBM will tell us something useful about the causes of polar amplification in the TRACMIP ensemble.

2.2 Calculation of instantaneous forcing, rapid adjustments, and feedbacks

Different methods are used to calculate the SW and LW components of radiative adjustments and feedbacks. For the SW, we use the Approximate Partial Radiation Perturbation method (APRP; Taylor et al. (2007)) to calculate the radiative effects of changes in cloud properties and in non-cloud atmospheric scattering and absorption. The latter is mainly due to SW absorption by water vapor, so we refer to this as the SW water vapor adjustment and feedback. For the LW, we use the aquaplanet radiative kernels developed by Feldl et al. (2017) to calculate the rapid adjustments and feedbacks associated with atmospheric temperature, surface temperature, and water vapor. We calcu-

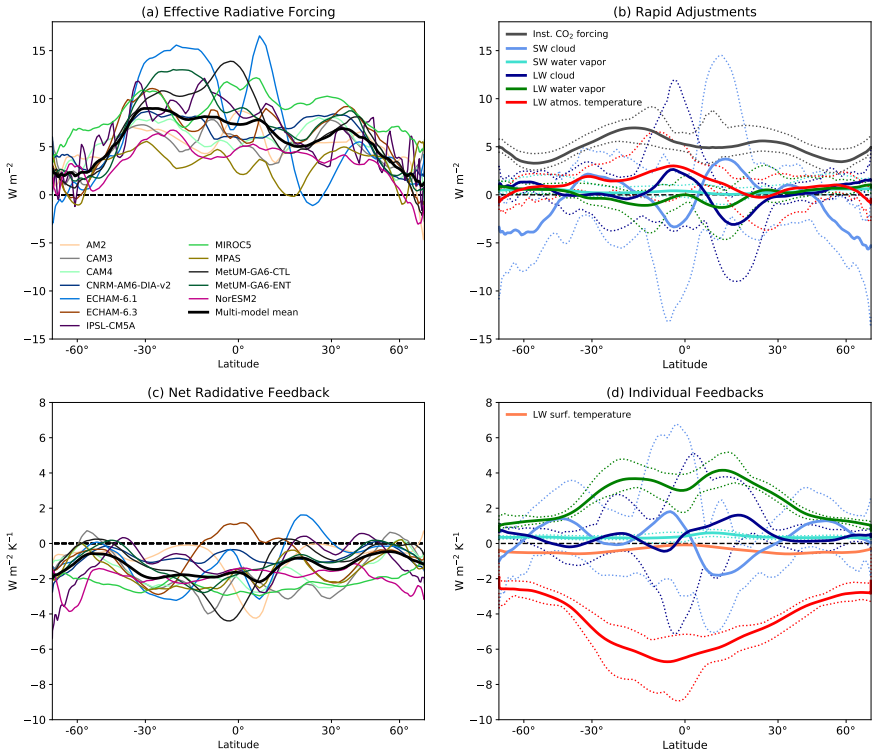

Figure 2. (a) Effective radiative forcing in each TRACMIP model. (b) Individual rapid adjustments and instantaneous CO_2 forcing: multi-model mean (solid curves) and maximum and minimum models (dotted curves in same colors). (c) Net radiative feedback in each TRACMIP model. (d) As in (b) but for individual radiative feedbacks.

late the LW radiative effects of changes in cloud properties by first taking the difference in outgoing longwave radiation between all-sky and clear-sky conditions, and then correcting for masking effects of pre-existing clouds by subtracting out the difference in TOA radiative flux change obtained from the clear-sky and all-sky versions of each of the LW radiative kernels. There is no aquaplanet radiative kernel for the CO_2 forcing, so we apply the correction for this term, the smallest contributor to cloud masking, based on full-geometry kernels (Shell et al., 2008; Soden et al., 2008). Finally, we estimate the instantaneous CO_2 radiative forcing by subtracting the sum of the rapid adjustments from the effective forcing.

The effective radiative forcing and its components are shown in Figure 2a and 2b, respectively. The effective radiative forcing is largest between 30°S and 30°N and decays towards the poles. This qualitative behavior is consistent across models, though inter-model spread is large. The physical reason for this pattern can be inferred from the individual components (Figure 2b). The instantaneous CO_2 forcing is relatively uniform across latitudes and has relatively little spread. The rapid adjustments are small by comparison to it, but exhibit much inter-model spread, particularly for the cloud adjustments. The SW cloud adjustment is negative in the poles for all models, resulting in the effective radiative forcing being weaker in the high latitudes than in the tropics.

The net feedback parameter (Figure 2c) is quite constant in latitude in the multi-model mean, but some individual models simulate a much more complex structure, with latitudinal differences of about 4 W m^{-2} K^{-1}. Among the individual feedbacks (Figure 2d), the water vapor feedback is consistently positive in all models, and stronger in the tropics, with the LW component being an order of magnitude stronger than the SW. The SW and LW cloud feedbacks vary in sign with latitude, and tend to be anticorrelated with each other; they are positive in the multi-model, global mean, but the inter-model spread surrounds zero at most latitudes and often exceeds that of the total net radiative feedback. The LW atmospheric temperature feedback, which includes the Planck and lapse rate feedbacks, is strongly negative, more so in the tropics. The surface temperature rapid adjustment is 0 by definition, and the surface temperature feedback reduces to the kernel, so it has no inter-model spread. However, we can still consider the effect of this weakly negative feedback on the multi-model mean response.

3 Results

Figure 3a,b shows the multi-model mean equilibrium temperature in each MEBM perturbation experiment. The rapid adjustments (Figure 3a) generally have less of an effect on the temperature change than the corresponding feedbacks (Figure 3b). On the other hand, turning off the instantaneous CO_2 forcing, leaving only the rapid adjustments to force the MEBM, completely eliminates the polar amplification (gray curve in Figure 3a). Polar amplification occurs in all of the feedback perturbation experiments, but it is weakened when the water vapor feedbacks are removed. Feedbacks involving clouds, which vary in sign with latitude, have the smallest effect on temperature in the multi-model mean.

The bottom 6 panels of Figure 3 show the contribution to warming at each latitude from each rapid adjustment, feedback, and the instantaneous forcing, obtained by taking the difference in the temperature anomaly from the control case and flipping the sign. As noted above, completely turning off the atmospheric temperature feedback would result in runaway warming, so the word "contribution" should not be taken literally in the case where this feedback is reduced by 10%. For the rapid adjustments (Figure 3c-3e), the inter-model spread is fairly small, but the cloud rapid adjustments might have an appreciable effect on polar amplification in the extreme cases. The instantaneous CO_2 forcing (Figure 3e) consistently contributes to polar amplification. Both the SW and LW cloud feedbacks (Figure 3f) have great inter-model uncertainty in their effect on polar amplification; they could either contribute to or detract from it depending on the sign of the overall temperature change. The water vapor feedback (Figure 3g), especially in the LW, tends to contribute to polar amplification, while the 10% perturbation of the atmospheric temperature feedback (Figure 3h), and similarly the surface temperature feedback (not shown), act in opposition to polar amplification by causing more cooling at the poles. In the extreme cases, however, these latter two cases may have little effect on the polar amplification. The positive and negative contributions to polar amplification by the water vapor and atmospheric temperature feedbacks, respectively, are counterintuitive, as these feedbacks are stronger in the tropics than at the poles (Figure 2d).

To further investigate the roles of the different rapid adjustments and feedbacks to tropical versus polar warming, Figure 4a shows a similar style of scatter plot to Figure 1 of Pithan and Mauritsen (2014), with contributions to tropical (30°S-30°N) warm-

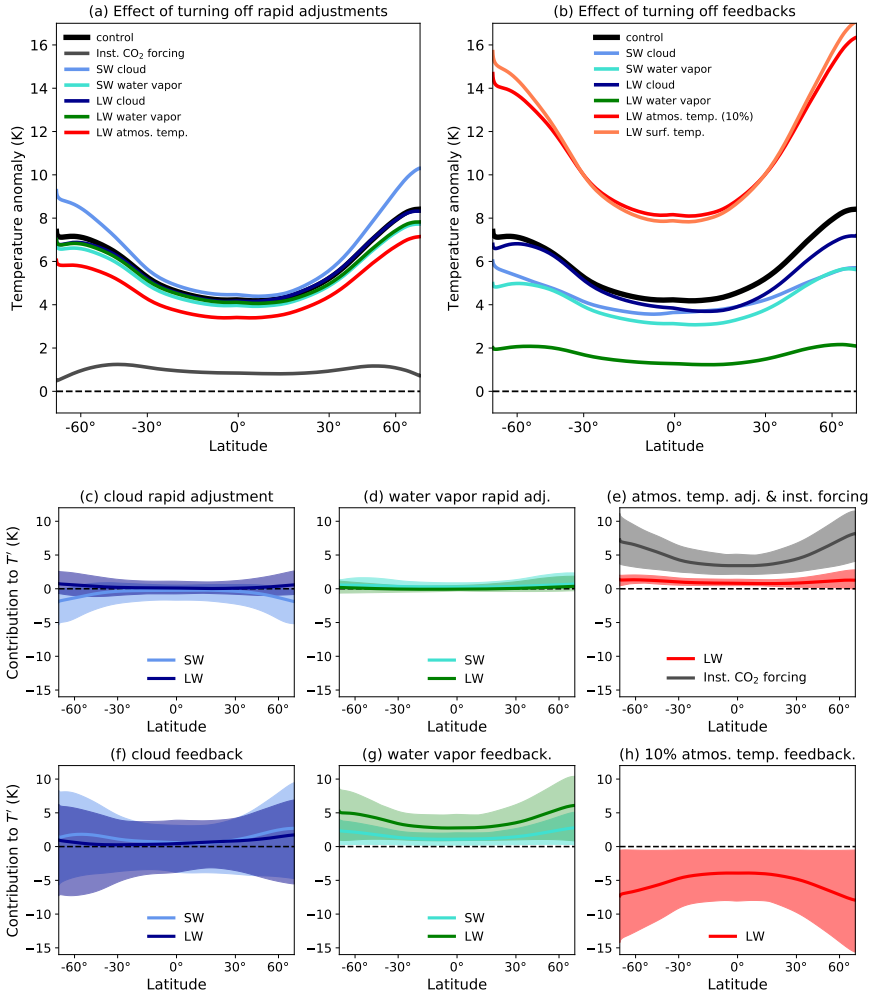

Figure 3. (a-b): Multi-model mean, MEBM-derived equilibrium zonal mean temperature anomalies in the control case (black) and perturbation experiments (colors). (c-h): Warming contribution associated with each forcing or feedback component (negative of the difference in warming from control), in the multi-model mean (curves) and range between maximum and minimum models (shaded areas).

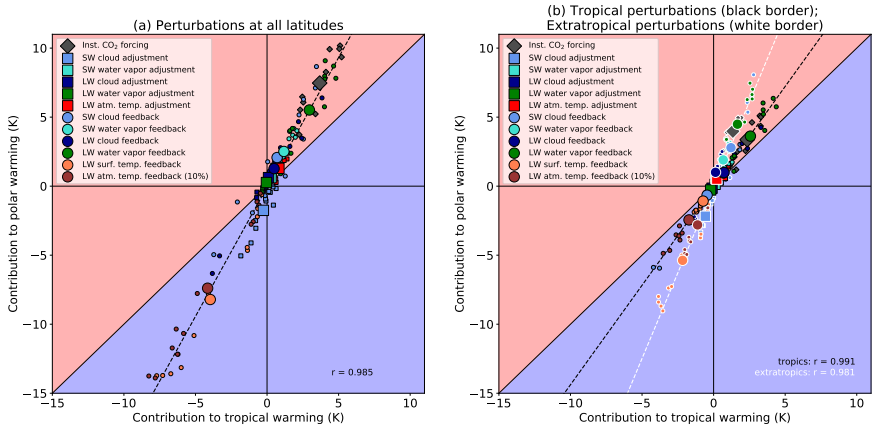

Figure 4. Contributions of each rapid adjustment, feedback, and the instantaneous CO_2 forcing to tropical (equatorward of 30 degrees) warming (x axis) and polar (poleward of 70 degrees) warming (y axis), for global (a) or tropical vs. extratropical (b) forcing and feedback perturbations. Large symbols are multi-model means; small symbols are results for individual models. Least squares regression fit lines (dashed) and correlation coefficients (r) calculated from the full set of runs from each model and experiment.

ing on the x-axis and contributions to polar (poleward of 70°) warming on the y-axis. Points above the 1:1 diagonal (pink background) indicate greater polar than tropical warming, *i.e.* the process contributes to polar amplification, while points below the diagonal (blue background) indicate processes that detract from polar amplification.

The most striking feature of Figure 4a is how linear the points are. A regression of the polar against the tropical warming contribution for each of the individual model-experiment pairs (shown as small symbols) has a very strong correlation, $r > 0.98$, with a least-squares best fit line (dashed) being steeper than the 1:1 line and passing very close to the origin. Very few points showing enhanced overall warming lie below the 1:1 line, while very few points showing diminished overall warming lie above it. Physically, this means that positive rapid adjustments and feedbacks contribute to polar amplification, while negative rapid adjustments and feedbacks oppose polar amplification. We can identify which processes contribute most strongly to polar amplification by looking at how far the multi-model means (large symbols) lie above the 1:1 line. The strongest contributor is the instantaneous CO_2 forcing, suggesting that polar amplification is an inherent response of the atmosphere to positive forcing and not primarily caused by any in-

dividual feedback or rapid adjustment. The strongest positive feedback—the LW water vapor feedback—is the next largest contributor, followed by the SW water vapor feedback, and the SW and LW cloud feedbacks, although the cloud feedback contributions might be on par with that of the water vapor feedback, or negative, depending on the model. The surface and atmospheric temperature feedbacks, and the SW cloud rapid adjustment, work against polar amplification in TRACMIP (but see the above caveat about the magnitude for the atmospheric temperature feedback). A 1-dimensional chart showing contributions to polar amplification is shown in Figure S1.

To help answer the question of whether local or nonlocal feedbacks are more important for polar amplification, we ran additional sets of MEBM experiments in which perturbations to R_f or λ were made only in the tropics (equatorward of 30°) or extratropics (poleward of 30°); these regions were chosen for simplicity and equal area. Contributions to tropical versus polar warming for these MEBM runs are shown in Figure 4b, with the tropical perturbation results having black symbol edges and the extratropical having white edges. The impacts on overall warming are smaller than in Figure 4a, expected given the smaller overall perturbations being applied, but each set of experiments still has a very linear set of responses, again with $r > 0.98$. The slope is steeper for the extratropical perturbations, indicating that feedbacks there more strongly effect polar amplification, consistent with Roe et al. (2015) and Stuecker et al. (2018). But positive feedbacks (and forcing components) still usually contribute to polar amplification even when only their tropical components are considered. This implies that, to the extent that the MEBM's treatment of MSE diffusion accurately captures the factors governing the meridional temperature gradient in the real world, analyses that presume to explain whether a feedback enhances or diminishes polar amplification on the sole basis of whether it is stronger in the tropics or poles are liable to give the wrong answer.

4 Discussion

The TRACMIP ensemble demonstrates that an ice-albedo feedback is not necessary to obtain polar amplification in most models in a GCM ensemble. Moreover, we have identified the instantaneous CO_2 forcing as the strongest contributor accounting for the existence of polar amplification in TRACMIP, followed by the water vapor feedback, with SW and LW cloud feedbacks also being important for some models. These amplifying factors work in opposition to a Planck feedback that weakens polar amplification. The

lapse rate feedback, which is negative at low latitudes but positive at high latitudes, may have a contribution to polar amplification which our methods could not identify, but in any case, this effect is masked by the always negative Planck feedback. The fact that the Caltech gray radiation model (O'Gorman & Schneider, 2008; Bordoni & Schneider, 2008), which lacks most of the physical processes responsible for the rapid adjustments and feedbacks, also exhibits polar amplification in TRACMIP (Voigt et al., 2016) further points to the primary role of the instantaneous CO_2 forcing in polar amplification.

It would be useful to use similar MEBM perturbation methods to break down the individual feedback contributions to polar amplification in a fully coupled GCM ensemble; we suspect that the water vapor feedback would still be found to have a positive contribution to polar amplification when considered this way, but the ice albedo feedback would also be important because it is positive and focused in high latitudes. The polar amplification in TRACMIP, while robust, is, at $<= 1.5$ (Figure 1f), much weaker than in the fully coupled CMIP5 equivalent (Figure S2), and ice-albedo feedback likely helps explain this difference in magnitude.

Our results, particularly regarding the role of the water vapor feedback, contradict those of past attempts to diagnose the causes of polar amplification. Studies making similar scatter plots to those in Figure 4 (Pithan & Mauritsen, 2014; Goosse et al., 2018; Stuecker et al., 2018) all describe the water vapor feedback as opposing polar amplification. Since these studies assume a 1:1 correspondence between TOA radiative changes and surface warming contributions, they do not account for interactions between the feedbacks and local temperature or MSE transport. On the other hand, Graversen and Wang (2009) cited the water vapor feedback as a reason for polar amplification in GCM experiments with fixed albedo, and our results support this conclusion. To shed further light on this discrepancy, we have run an alternative set of EBM experiments in a configuration that diffuses only dry static energy. This eliminates the polar amplification in the control case (Figure S3), and the water vapor radiative feedback now opposes polar amplification in the multi-model mean (Figure S4), indicating that latent heat transport plays a critical role in polar amplification and in the effect of individual feedbacks on it.

Eliminating the moisture transport recaptures some of the north-south warming asymmetry seen in the GCMs (*cf.* Figures 1 and S3), suggesting that the MEBM misses

some important aspects of the warming pattern by diffusing too much latent heat out of the tropics in both directions. More generally, the very strong linearity shown in Figure 4 might seem "too good to be true", suggesting we should be cautious about extrapolating results from such a simple model to the real, vastly more complex Earth. These caveats motivate the possibility of applying similar "mechanism denial" methods to study polar amplification in a more comprehensive GCM context. Others have already perturbed individual forcings and feedbacks in comprehensive GCMs to study polar amplification, such as applying CO_2 forcing in specific latitude bands (Stuecker et al., 2018), or eliminating the ice-albedo feedback (Alexeev et al., 2005; Graversen & Wang, 2009), interactivity of sea ice with the ocean (Dai et al., 2019), or cloud-radiation interactions (Stevens et al., 2012). A multi-GCM study perturbing *all* relevant feedbacks would be a major and difficult undertaking, but it might be necessary to resolve the disagreements over the causes of polar amplification obtained from limited GCM experiments and different diagnostic techniques.

Acknowledgments

The authors and the TRACMIP project are supported by NSF award AGS-1565522. We thank Nicole Feldl for assistance with using the aquaplanet radiative kernels and Lorenzo Polvani for helpful discussions. We acknowledge the work of the TRACMIP modelers (listed in Voigt et al. (2016)) in generating, curating, and making available the model output. The TRACMIP output has been uploaded to the Earth Science Grid Federation repository at `https://esgf-data.dkrz.de/search/esgf-dkrz/`, in a format consistent with the Climate Model Output Rewriter conventions. IPython notebooks used to analyze data and make plots are uploaded to `https://github.com/rdrussotto/TRACMIP_pa_notebooks`. These will be transferred to a permanent repository upon acceptance of the paper.

References

Alexeev, V. A., Langen, P. L., & Bates, J. R. (2005). Polar amplification of surface warming on an aquaplanet in "ghost forcing" experiments without sea ice feedbacks. *Climate Dynamics*, *24*(7), 655–666. doi: 10.1007/s00382-005-0018-3

Armour, K. C., Siler, N., Donohoe, A., & Roe, G. H. (2019). Meridional atmospheric heat transport constrained by energetics and mediated by large-scale diffusion.

Journal of Climate, *32*(12), 3655-3680. doi: 10.1175/JCLI-D-18-0563.1

Bonan, D. B., Armour, K. C., Roe, G. H., Siler, N., & Feldl, N. (2018). Sources of uncertainty in the meridional pattern of climate change. *Geophysical Research Letters*, *45*(17), 9131-9140. doi: 10.1029/2018GL079429

Bordoni, S., & Schneider, T. (2008). Monsoons as eddy-mediated regime transitions of the tropical overturning circulation. *Nature Geoscience*, *11*, 515–519. doi: 10.1038/ngeo248

Dai, A., Luo, D., Song, M., & Liu, J. (2019). Arctic amplification is caused by sea-ice loss under increasing CO2. *Nature Communications*, *10*(121). doi: 10.1038/s41467-018-07954-9

Feldl, N., Bordoni, S., & Merlis, T. M. (2017). Coupled high-latitude climate feedbacks and their impact on atmospheric heat transport. *Journal of Climate*, *30*(1), 189-201. doi: 10.1175/JCLI-D-16-0324.1

Feldl, N., & Roe, G. H. (2013). Four perspectives on climate feedbacks. *Geophysical Research Letters*, *40*(15), 4007-4011. doi: 10.1002/grl.50711

Flannery, B. P. (1984). Energy balance models incorporating transport of thermal and latent energy. *Journal of the Atmospheric Sciences*, *41*(3), 414-421. doi: 10.1175/1520-0469(1984)041⟨0414:EBMITO⟩2.0.CO;2

Frierson, D. M. W., & Hwang, Y.-T. (2012). Extratropical influence on ITCZ shifts in slab ocean simulations of global warming. *Journal of Climate*, *25*(2), 720-733. doi: 10.1175/JCLI-D-11-00116.1

Goosse, H., Kay, J. E., Armour, K. C., Bodas-Salcedo, A., Chepfer, H., Docquier, D., ... Vancoppenolle, M. (2018). Quantifying climate feedbacks in polar regions. *Nature Communications*, *9*(1919). doi: 10.1038/s41467-018-04173-0

Graversen, R. G., & Wang, M. (2009). Polar amplification in a coupled climate model with locked albedo. *Climate Dynamics*, *33*(5), 629–643. doi: 10.1007/s00382-009-0535-6

Gregory, J. M., Ingram, W. J., Palmer, M. A., Jones, G. S., Stott, P. A., Thorpe, R. B., ... Williams, K. D. (2004). A new method for diagnosing radiative forcing and climate sensitivity. *Geophysical Research Letters*, *31*(3), L03205. doi: 10.1029/2003GL018747

Hall, A. (2004). The role of surface albedo feedback in climate. *Journal of Climate*, *17*(7), 1550-1568. doi: 10.1175/1520-0442(2004)017⟨1550:TROSAF⟩2.0.CO;2

Hwang, Y.-T., & Frierson, D. M. W. (2010). Increasing atmospheric poleward energy transport with global warming. *Geophysical Research Letters*, *37*(24), L24807. doi: 10.1029/2010GL045440

Hwang, Y.-T., Frierson, D. M. W., & Kay, J. E. (2011). Coupling between arctic feedbacks and changes in poleward energy transport. *Geophysical Research Letters*, *38*(17), L17704. doi: 10.1029/2011GL048546

Merlis, T. M., & Henry, M. (2018). Simple estimates of polar amplification in moist diffusive energy balance models. *Journal of Climate*, *31*(15), 5811-5824. doi: 10.1175/JCLI-D-17-0578.1

Myhre, G., Shindell, D., Bréon, F.-M., Collins, W., Fuglestvedt, J., Huang, J., ... Zhang, H. (2013). Anthropogenic and natural radiative forcing [Book Section]. In T. Stocker et al. (Eds.), *Climate change 2013: The physical science basis. contribution of working group i to the fifth assessment report of the intergovernmental panel on climate change* (p. 659–740). Cambridge, United Kingdom and New York, NY, USA: Cambridge University Press. Retrieved from `www.climatechange2013.org` doi: 10.1017/CBO9781107415324.018

North, G. R., Cahalan, R. F., & Coakley Jr., J. A. (1981). Energy balance climate models. *Reviews of Geophysics*, *19*(1), 91-121. doi: 10.1029/RG019i001p00091

O'Gorman, P. A., & Schneider, T. (2008). The hydrological cycle over a wide range of climates simulated with an idealized GCM. *Journal of Climate*, *21*(15), 3815-3832. doi: 10.1175/2007JCLI2065.1

Pithan, F., & Mauritsen, T. (2014). Arctic amplification dominated by temperature feedbacks in contemporary climate models. *Nature Geoscience*, *7*, 181–184. doi: 10.1038/NGEO2071

Roe, G. H., Feldl, N., Armour, K. C., Hwang, Y.-T., & Frierson, D. M. (2015). The remote impacts of climate feedbacks on regional climate predictability. *Nature Geoscience*, *8*, 135–139. doi: 10.1038/NGEO2346

Shell, K. M., Kiehl, J. T., & Shields, C. A. (2008). Using the radiative kernel technique to calculate climate feedbacks in ncar's community atmospheric model. *Journal of Climate*, *21*(10), 2269-2282. doi: 10.1175/2007JCLI2044.1

Siler, N., Roe, G. H., & Armour, K. C. (2018). Insights into the zonal-mean response of the hydrologic cycle to global warming from a diffusive energy

balance model. *Journal of Climate*, *31*(18), 7481-7493. doi: 10.1175/JCLI-D-18-0081.1

Soden, B. J., Held, I. M., Colman, R., Shell, K. M., Kiehl, J. T., & Shields, C. A. (2008). Quantifying climate feedbacks using radiative kernels. *Journal of Climate*, *21*(14), 3504-3520. doi: 10.1175/2007JCLI2110.1

Stevens, B., Bony, S., & Webb, M. (2012). *Clouds on-off klimate intercomparison experiment (COOKIE).* ([Available online at `https://pure.mpg.de/rest/items/item_2078839/component/file_2079076/content`])

Stuecker, M. F., Bitz, C. M., Armour, K. C., Proistosescu, C., Kang, S. M., Xie, S.-P., ... Jin, F.-F. (2018). Polar amplification dominated by local forcing and feedbacks. *Nature Climate Change*, *8*, 1076–1081. doi: 10.1038/s41558-018-0339-y

Taylor, K. E., Crucifix, M., Braconnot, P., Hewitt, C. D., Doutriaux, C., Broccoli, A. J., ... Webb, M. J. (2007). Estimating shortwave radiative forcing and response in climate models. *Journal of Climate*, *20*(11), 2530-2543. doi: 10.1175/JCLI4143.1

Taylor, K. E., Stouffer, R. J., & Meehl, G. A. (2012). An overview of CMIP5 and the experiment design. *Bulletin of the American Meteorological Society*, *93*(4), 485-498. doi: 10.1175/BAMS-D-11-00094.1

Vavrus, S. (2004). The impact of cloud feedbacks on arctic climate under greenhouse forcing. *Journal of Climate*, *17*(3), 603-615. doi: 10.1175/1520-0442(2004)017⟨0603:TIOCFO⟩2.0.CO;2

Voigt, A., Biasutti, M., Scheff, J., Bader, J., Bordoni, S., Codron, F., ... Vargas Zeppetello, L. R. (2016). The tropical rain belts with an annual cycle and a continent model intercomparison project: TRACMIP. *Journal of Advances in Modeling Earth Systems*, *8*(4), 1868-1891. doi: 10.1002/2016MS000748